Determination of Flow in an Axial-to-Radial Diffuser with Swirl

by

Robert Allen Major

Thesis Supervisor: David G. Wilson
Submitted: May 17, 1968

DETERMINATION OF FLOW IN AN AXIAL-TO-RADIAL DIFFUSER WITH SWIRL

by

ROBERT ALLEN MAJOR
LIEUTENANT, UNITED STATES COAST GUARD
B.S., United States Coast Guard Academy
(1963)

Submitted in Partial Fulfillment of the
Requirements for the Degree of
Naval Engineer and the Degree of
Master of Science in Mechanical Engineering
at the
MASSACHUSETTS INSTITUTE OF TECHNOLOGY
May, 1968

DETERMINATION OF FLOW IN AN AXIAL-TO-RADIAL DIFFUSER WITH SWIRL

by

ROBERT ALLEN MAJOR

Submitted to the Departments of Naval Architecture and Marine Engineering and of Mechanical Engineering on May 17, 1968 in partial fulfillment of the requirements for the Master of Science degree in Mechanical Engineering and the Professional Degree, Naval Engineer.

ABSTRACT

The parameters affecting the efficient design of axial-to-radial diffusers are discussed and a selection made of those to be investigated. A model diffuser was constructed based on the geometry of a jet impinging on a flat plate without internal vanes. Various amounts of swirl were introduced on a constant flow rate and the recovery of the diffuser for these conditions noted. The internal flow was mapped photographically and with pressure probes.

The results are given in the form of static pressure plots along the diffuser walls, velocity profiles, and calculated diffuser efficiency. The maximum efficiency of 91.7% occured at just under the maximum swirl used, based on a calculated inlet pressure.

A detailed program for additional testing is given.

Thesis Supervisor: D. G. Wilson

Title: Associate Professor of Mechanical Engineering

ACKNOWLEDGEMENTS

First, I would like to thank the U.S. Coast Guard for sponsoring my studies here at M.I.T. and this thesis.

I am indebted to Prof. David G. Wilson, my thesis supervisor, for his close attention to the progress of this work and his many helpful suggestions. Also other members of the staff of the M.I.T. Gas Turbine Laboratory and students working there helped with useful comments both at seminars and in the laboratory.

Mr. Thorwald Christiansen was very helpful with the construction of the apparatus.

Finally, I would like to thank Mrs. Jutta Budek for her quick and efficient typing.

TABLE OF CONTENTS

LIST OF FIGURES

LIST OF SYMBOLS

A	area
c	velocity
D	diameter
g	gravity
h	manometer, height
l	distance along curved wall from inlet
L	non-dimensional distance along wall, $\frac{l}{r_{in}}$
p	pressure
r	radial cylindrical coordinate
R	non-dimensional radius, $\frac{r}{r_{in}}$
T	atmospheric temperature
w	weight density
x	axial cylindrical coordinate
X	non-dimensional distance from flat plate $\frac{x}{x_{max}}$
α	inlet angle
$\triangle$	change in . . .
θ	angular cylindrical coordinate
μ	viscosity
η	efficiency
ρ	mass density
C_D	discharge coefficient
Re	Reynolds number based on inlet diameter.

SUBSCRIPTS

a	atmospheric
r	radial component
x	axial component
in	inlet
max	maximum value
out	outlet
wall	inlet wall
1,2	points on a streamline
—	average value
θ	angular component

I. INTRODUCTION

USES OF RADIAL DIFFUSERS

To date there has been little experimental work which would be applicable to axial-to-radial diffusers. This type of diffusers would be used, for instance, on radial-inflow turbines as an exhaust diffuser. The radial-inflow turbine shows promise as the power turbine for transportation applications where its compactness, high starting torque, and relative ease of reversing would be of more importance than the slightly lower efficiency compared to an axial power turbine. In marine use, such a device would allow reversing of propeller rotation with a gas-turbine prime mover. This is possible with diesel and steam plants now; however, gas-turbine plants must use electric drive, a controllable pitch propeller, or a reversing gear to reverse thrust, all of which decrease the weight advantage of the gas turbine. For a railroad, it might be possible to place reversible turbines on the trucks, eliminating complex gearing or electric drive. Large trucks or tanks could use reversible turbines in lieu of a gearbox.

DESIGN NEED

Why is a diffuser needed? The exducer of a turbine rotor can be designed for zero swirl in one direction only. Thus there will be a high degree of swirl in at least one direction of rotation. This swirl must be reduced for maximum efficiency. Conical diffusers do not accomplish this well. A compact design would use a radial diffuser. For a radial-inflow machine, an axial diffuser inlet is required. Design data for such a diffuser are apparently nonexistent.

PREVIOUS WORK

There has been some work on diffusers which would be particularly applicable to radial-outflow machines, such as radial or mixed-flow compressors. Early N.A.C.A. experiments by W. Byron Brown and Guy R.

Bradshaw attempted to design on the basis of a log spiral with one dimensional flow (1). Their results were explained by using abnormally high friction coefficients to account for the wakes and unsteady flow which they must have had. The internal flow field of the diffuser was not studied. Willem Jansen did some work on a parallel-plate diffuser at the M.I.T. Gas Turbine Laboratory in 1959 - 60 (2). He identified four separate factors which contribute to pressure loss in a vaneless diffuser. They are: 1.) wakes, 2.) boundary-layer growth, 3.) unsymmetric flow with respect to the mid-point between two walls, and 4.) other unsteady flow. Isolating case 2.) above, he successfully predicted the boundary-layer growth in an axially symmetric flow field, but he encountered problems in unsteady and unsymmetrical flow. More recently Ronald C. Pampreen of Wayne State University conducted an axi-symmetrical analysis for a constant-area diffuser (5). He determined for a laminar boundary layer that, up to a radius of 1.15 times the inlet radius, the constant-area diffuser is better than the parallel-plate diffuser; however there was no experimental verification. In an experiment at Nagoya Institute of Technology, Japan, Tatsuji Kawaguchi and Yoshimasa Furuya used a water apparatus to verify their prediction of the three-dimensional boundary layer in a parallel-plate diffuser with axi-symmetric flow (3). A.N. Sherstyuk and A.C. Sokolov in recent Russian experiments have shown that a reduction of diffuser width at the inlet of some twenty per cent on the shroud side increased efficiency some three to four per cent (7). All of these experimenters concerned themselves with devices with a radial inlet, as is found at the outlet of a pump or compressor.

In experiments with axial-to-radial diffusers without swirl, O. Ruchti in Germany found that the use of a centerbody actually reduced the efficiency of his diffusers (6). Garrett Airesearch noted great improvement in their reversible turbine performance when an exhaust diffuser was added (4). However, there seems to have been little engineering or testing of the diffuser design itself. The report notes that more data are needed in this area.

DESIGN PARAMETERS

A first step in an experimental program is the identification of the parameters affecting the design. For an axial-to-radial diffuser these choices are: shape, centerbody, turning vanes, entering wakes, turbulence, swirl, inlet boundary layer, radius ratio, and similarity.

First, there is the geometry of the walls. They must diverge with respect to the stream lines or no diffusion will take place. However this does not mean that the meridional profile must also diverge. A constant-area geometry will also diffuse a swirling flow, while the meridional profile actually contracts. To prevent vortex cells from forming, centerbodies are sometimes added. There is the possibility of having either axially symmetric turning vanes or a cascade of turning vanes. Axially symmetric vanes could handle a range of swirl but would complicate the design. A cascade of turning vanes could be designed for one swirl angle only unless they were adjustable. Either type of turning vane would cause wakes if it ended within the diffuser. Entering wakes from the machine on which the diffuser is used would also affect performance. The level of turbulence in the diffuser will change effectiveness. The amount of swirl to be handled will affect the choice of geometry. An inlet-boundary layer will decrease the effective area of the diffuser. The radius ratio in a gas-turbine design will probably be limited by the turbine radius ratio; but it is possible that a smaller radius ratio might be just as effective. In a model it is desirable to have as many similarity parameters as possible in the same range as those in the actual device. The most important ones are Reynolds number and Mach number in a diffuser. These parameters are studied and a selection made of those to be investigated.

The apparatus for study of the flow field was constructed and the experimental program begun. The results of this thesis when combined with subsequent work suggested will show how swirl angle, radius ratio, and flow rate affect the pressure recovery of an axial-to-radial diffuser. A study of the boundary-layer growth when compared with other studies should suggest the most efficient geometrical form.

II. PROCEDURE

SELECTION OF PARAMETERS

The first problem was the selection of the variables to be investigated and their ranges. Air was chosen as the fluid to permit elimination of a recirculation loop and allow simpler construction.

We decided to choose as a typical radial turbine for which we would model our tests a machine with a four-inch-diameter exhaust at 1200°F and velocity at the maximum diameter of 1000 ft./sec. in the angular direction and 578 ft./sec. (a 30° angle) in the radial direction. The wall shape was taken from an incompressible jet impinging on a flat plate. This shape was determined electrolytically by A. Le Clerc at Iowa State University and is reproduced here as Figure I. When there is no swirl the curved-wall streamline is one of constant velocity and constant pressure. The cross section of the diffuser becomes one of constant area as the streamline curvature becomes large - i.e. as the flow becomes more nearly parallel to the back plate. Referring to Figure I, the section used was that from $y/r_o = 2$ to $r/r_o = 4$. This last value, which is the maximum radius divided by the inlet radius I will call radius-ratio. Construction of the apparatus was done with future reduction of this radius ratio in mind. The outer section of the diffuser can eventually be cut off in steps leaving a radius-ratio of 3.33. No centerbody, turning vane, or cascade, was added between the walls due to the added complexity. Entering wakes were eliminated through the use of flow-smoothing screens. The swirl was created by using a rotating screen which gave small, finely-distributed wakes that were quickly dispersed. The screen was far upstream of the test section and a converging section between the screen and the test section kept the boundary-layer from growing large. Turbulence was kept as small as possible. Swirl was varied by rotating the inner of two screens at different speeds using a variable-speed motor. The test apparatus was three times the size of the hypothetical diffuser for the typical radial turbine. For Reynolds similarity this makes the velocities lower and easier

to handle. Mach effects were not to be modeled correctly.

CONSTRUCTION

I built the diffuser with a solid curved wall of plywood, plaster, and wax. To allow visual examination of the flow, and photography, I made the flat-plate portion of the diffuser out of acrylic plastic. A plenum surrounded the curved-wall portion of the diffuser and was the support for the flat-plate. The plenum was connected to an induced-draft fan. The rotating screen and entrance were also outside of the plenum. Details of the actual construction are given in Appendix A. Photographs of the apparatus are Figures II - V. Plans are given in Figure VI.

INSTRUMENTATION

The two parameters varied were amount of swirl and mass flow rate. The swirl was changed by changing the speed of a variable-speed motor. This speed was adjusted with a rheostat and was calibrated for speed. The calibration was checked with a watch, and thereafter swirl measured with motor speed. The mass flow rate was varied through use of a valve at the plenum outlet.

It was desirable to know the flow rate without integrating a velocity profile in the diffuser. For this reason a settling chamber and venturi cone was placed downstream of the induced-draft fans. A honeycomb just upstream of the cone eliminated swirl in the flow. The flow from the cone was measured with a pitot traverse, integrated over the area of the duct. From this traverse the discharge coefficient of the cone could be calculated from a pressure tap at the cone entrance. At the velocities involved the flow could be considered incompressible. From the discharge coefficient so obtained, the flow rate could be measured with good accuracy using just one pressure tap. The integration of the exit profile shows a difference between the mass flow measured by the cone and that of the integrated profile of 7.4%.

Pressure measurements were made both with static taps and probes. See the sketch below of measuring devices.

Static taps were placed every two inches along both the curved and flat surfaces. The inlet profile was taken using a Keil probe for the total pressure and a Prandtl tube for the static pressure. The Prandtl tube could not be aligned perfectly with the flow due to the three-dimensional nature of the flow, so the Keil probe was used for its insensitivity to angle of attack.

SKETCH I

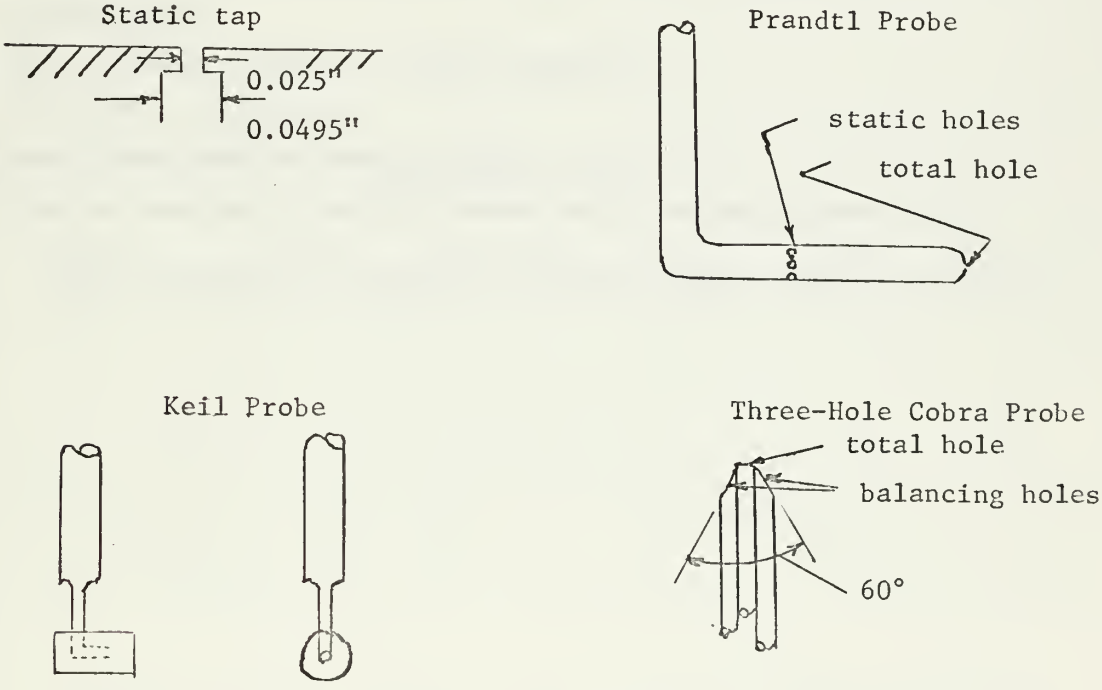

The outlet profile and intermediate profiles were taken using a traversing mechanism and a three-hole cobra probe to determine both angle and total pressure.

Tufts of thread were used to visualize the flow. The boundary-layer flow direction was determined by placing tufts at two-inch intervals, and then photographing them. A thread probe was used to see the direction of flow before measuring it with a pressure probe. Water injected in the boundary layer was also used to visualize flow.

TEST PROCEDURE

A typical data-taking sequence was as follows:

1. Set screen speed.
2. Start a combination of induced draft fans.
3. Check mass flow using venturi cone and current atmospheric pressure and temperature.
4. Adjust valve.
5. Re-check mass flow and repeat adjustments until desired flow rate is obtained.
6. Zero manometer board on plenum pressure.
7. Read static pressures.
8. Take photograph of boundary-layer tufts.
9. Measure internal flow with probes using traversing mechanism.

This was done for one flow rate and varying amounts of swirl.

III. RESULTS

The results of experiments on the model are in the form of static-pressure plots, velocity profiles, and photographs. Appendix B contains a sample of the data.

PRESENTATION OF DATA

The static-pressure plots show the static pressure along the wall non-dimensionalized on the inlet dynamic pressure. For each of the differing amounts of swirl, the mass-flow rate was adjusted to the same constant value. Figures VII - XIV show the non-dimensional static pressure at the wall as a function of the radius, and as a function of distance from the inlet. What is desired is the greatest transformation of the inlet dynamic pressure to static pressure. This varies with the swirl angle. The inlet swirl angle was obtained from a measurement of the total velocity at the inlet away from the boundary layer at R = 0.66 and the bulk axial velocity. Inlet swirl angle was then correlated to the screen velocity which in turn varied directly with the drive motor rpm.

Velocity profiles were obtained at the inlet and outlet, and at a few intermediate points. An inlet profile is given in Figure XV, and an outlet profile in Figure XVI.

Photographs of tufts attached to both the flat plate and curved wall were taken at varying swirls. Some of these are shown in Figures XVII to XX.

DIFFUSER EFFICIENCY

Diffuser efficiency is defined here as the actual pressure recovery divided by that which would be obtained if all of the swirl velocity were converted to static pressure. Efficiency varied from zero

at no swirl to a maximum value of 91.7%. A plot of efficiency vs. swirl angle is shown in Figure XXI.

OTHER OBSERVATIONS

Water droplets were injected into the boundary layer on either wall. These drops showed separation lines on the flat plate at two points better than the tufts had showed them. It appeared that the flow in the diffuser was unsteady, which was noted because the tufts oscillated more than normal self-excitation in a turbulent flow would show. Water droplets were injected through static-pressure taps to slow the mean flow at the wall. The water droplets injected inside a radius R = 1.17 on the flat plate migrated to R = 0.5 at a swirl α = 22.3°. Those injected on the curved surface and on the flat plate outside R = 1.17 migrated outward with the flow. The migration showed existence of at least one separated region of flow and possibly more. Possible cell patterns are shown below.

SKETCH II

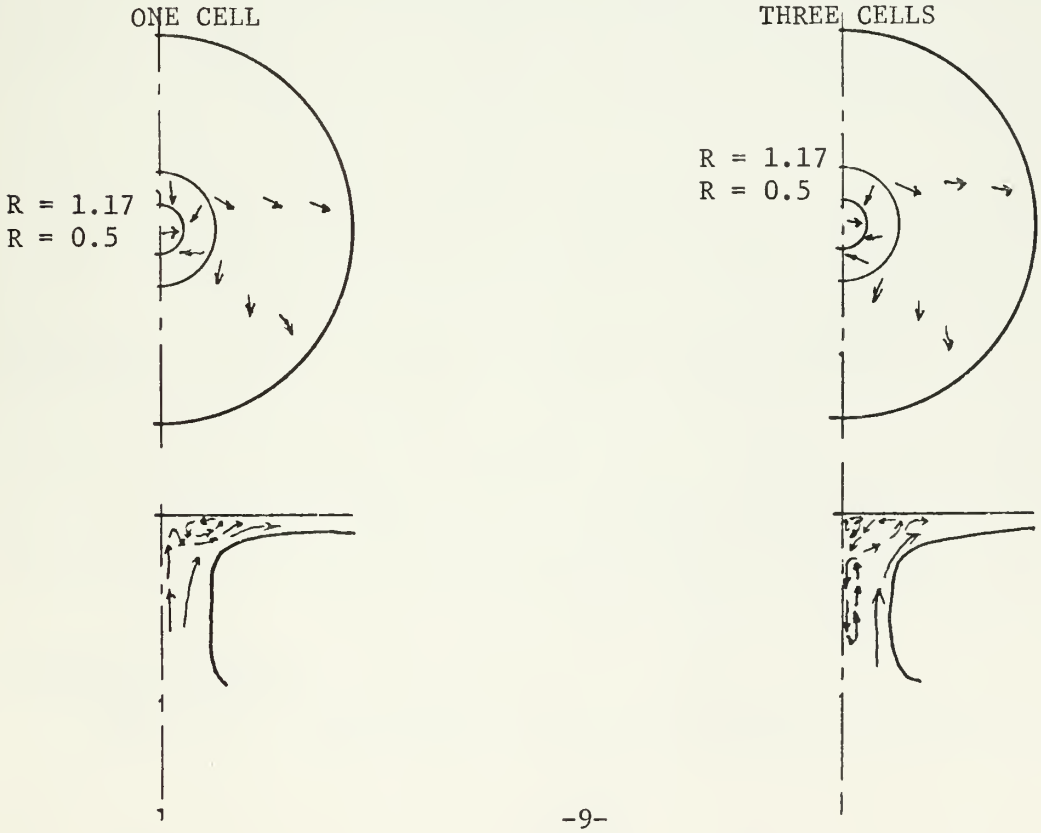

When the mass-flow rate was extremely small, a rotating stall could be observed by noting the change in flow direction on the tufts of thread. None of the data was taken when this flow pattern existed.

Sample calculations used to interpret the data are found in Appendix C.

IV. DISCUSSION OF RESULTS

The purpose of using a curved wall giving decreasing diffuser width was to delay separation. Since the pressure gradient is radial while the flow is not in this direction, there will exist a skewed boundary layer. The decreasing width is in the direction of the pressure gradient, and thus should reduce the difference in angle between that of the "main" flow and that of the boundary layer at the wall.

PRESSURE PROFILES

Separation did not occur due to a skewed boundary layer in the outer section of the diffuser. However, unsteady flow phenomena, and the existence of stall cells near the centerline axis, undoubtedly decreased efficiency. The presence of the stall cell is easily seen on the pressure profile. In steady flow of this geometry the pressure profile on the flat plate would be a smooth curve with its lowest pressure occurring at the centerline. Figures IX - XIV show a pronounced bump in the pressure curve on the flat plate where the stall cell existed. The higher pressure at the larger radius forced the boundary layer to flow inward creating the stalled region observed.

The curved-surface pressure profile shows a rise in pressure just beyond the inlet followed by a progressively decreasing pressure to a low point at the region of maximum curvature. Observations of the boundary layer showed that no stall cell existed on the curved surface. The low pressure observed is due to the curvature of the streamlines at this point as well to a reduction in the flow area due to the stall on the opposite wall. The short increasing pressure at the inlet is probably due to some diffusion taking place in this region.

VELOCITY PROFILES

There was a considerable problem in determining the inlet profile

and efficiency. The inlet was accessible for measurement only at three points. Probe access holes in the flat plate at R = 0.33, R = 0.67, and R = 1 allowed probes to be extended 12 inches through the flow to the inlet. The inlet angle could not be measured directly, since it was impossible to align the probes exactly with the flow. Thus only three velocities across the inlet could be measured and direction could not be determined for these. Since the flow in the inlet is in the nature of a vortex, the static pressure across the inlet is not constant, but is a maximum at the wall and a minimum at the solid-body core of the vortex. Thus the wall pressure is not satisfactory as a measure of inlet pressure. Figures VII - XIV show that the outlet wall pressure is lower than the inlet wall pressure. Some means must be devised to get a meaningful inlet pressure. The inlet pressure was obtained by reducing the wall pressure by an amount equal to the difference in the dynamic pressure measured at the wall and that measured in the main flow to get an approximate inlet pressure. The outlet pressure was simply the plenum chamber pressure. The efficiency was then the difference between the inlet and outlet pressures divided by the dynamic pressure of the inlet swirl. The diffuser efficiency reached a maximum of around 92% which is the same efficiency obtained by Jansen in steady flow (1).

The outlet was much more accessible than the inlet, and thus a traversing mechanism could be used. A three-hole cobra probe was used to obtain simultaneous total-pressure and direction readings. The skew in the outlet profile was considerably less than expected. The boundary-layer direction differed only a few degrees from the main flow (see Appendix B).

PHOTOGRAPHS

I expected the tufts in the boundary layer to be easily measured to determine flow direction. However, due to the unsteadiness of the flow, the tufts vibrated so much that angle was nearly impossible to measure, at least to any accuracy. The tufts do give an idea of the overall flow field though.

EFFICIENCY

The efficiency was based on a very rough approximation of the inlet pressure obtained as described under "Velocity Profiles" earlier. I do not give it much credit for quality. The efficiency did seem to reach a peak near the maximum swirl used.

IMPROVEMENTS ON EXISTING APPARATUS

The most pressing need is for an accurate measurement of the inlet velocity profile, both in amplitude and direction. An accurate measurement can only be obtained by making a traverse across the inlet by cutting a hole in the side wall of the diffuser. It is impossible to say with conviction that the diffuser is good when only three rough measurements determined the inlet profile. With an accurate profile, an integrated enthalpy could be obtained for the inlet, which when outlet enthalpy was subtracted would be a more accurate index of performance.

A first attempt at reducing the unsteadiness in the flow would be some reinforcement of the flat-plate section. Since the diffuser operates in the apparatus below atmospheric pressure, and atmospheric pressure exists on one side of the acrylic plastic plate, there is bound to be some deflection. At the maximum swirl used, the deflection of this plate at the center was 0.250 inches. This is a considerable amount, considering that if this were 0.15 inches at R = 1.67, this would be a 7.5% decrease in area. This adds to the unfavorable pressure gradient in the part of the diffuser where the walls get closer and the boundary layer is more important. The vibration in this large unsupported plate may be sufficient in amplitude to induce velocities that trip the boundary layer into the stalled regions although it will have a negligible effect on pressure readings. Thus simply making the plate stiffer may eliminate some of the stall and increase efficiency.

I ran out of time to do a complete mapping of the internal flow field. The access is already provided for traverses to be made. Knowing the extent and number of stall cells would help in choice of some centerbody to help eliminate them. It would also be desirable to know the

extent of the unsteadiness in the flow. Hot-wire measurements should be made to try to determine the source of any unsteadiness and eliminate it.

Only one flow rate was used in my tests. The apparatus could easily be run at a lower flow rate to see if inlet angle is really the variable which most affects performance as both Jansen and Pampreen assert (1,5). With the use of the hot wire it might be possible to determine a limiting inlet angle beyond which unsteady flow exists.

CHANGES IN PRESENT APPARATUS

After the tests mentioned above are completed, the present apparatus could be modified for still other tests. The flow rate at present is just below that required for Reynolds similarity with the hypothetical gas-turbine envisioned. A new fan with a greater pressure rating could increase the flow rate for another series of tests at a higher flow than similarity dictates. Perhaps with higher flow rate the boundary layer will be thinner and the diffuser more efficient.

I originally intended cutting the radius ratio down by two successive steps. In an actual machine the radius would be limited by the turbine radius for compact packaging. There will be, however, an optimum radius for recovery of pressure, which will probably be larger than the machine allows. Reduction of the test-apparatus radius will show how much efficiency is gained or lost by having a smaller diffuser. Friction will be lower for the smaller diffuser, but this is usually a small loss in diffusers anyway. To reduce the radius will require a new support for the acrylic plastic plate each time, but this would be a relatively simple job. The curved wall can be cut all at once with a sabre saw.

Another modification to the present apparatus would be the inclusion of a centerbody. It appears that the 90° change of flow direction is a serious cause of separation. A centerbody to increase the velocity in the vicinity of the present stalled region might improve performance more than it blocked the flow.

NEW APPARATUS

Other shapes will also have to be investigated. Perhaps after the flow has been turned there is a point at which beginning a parallel-plate diffuser would be advantageous. There is also the possibility of choosing any of the other streamline shapes given in Figure I. Shapes outside the free-stream boundary turn the flow faster but are more liable to have an adverse pressure gradient at the narrowest width of the diffuser. Conversely shapes inside of the free-stream boundary turn the flow more slowly, and have their adverse pressure gradient more in the large inlet.

With the completion of this exhaustive test program there should be accumulated a large body of knowledge from which it would be possible to draw the design of the most efficient vaneless axial-to-radial diffuser.

V. CONCLUSIONS

The tests conducted are only the first step in a comprehensive program for axial-to-radial diffusers. Thus the conclusions are at best preliminary.

The optimum inlet angle for this geometry appears to be 23°, for which an efficiency of 92% is realized. Unsteady flow and stall cells exist within the diffuser. The decreasing diffuser width with radius appears to delay separation. Rotating stall does not appear to exist, but this would have to be checked by hot-wire measurement. The formation of stall cells in the center of the diffuser is caused by a combination of the presence of the vortex, sharp change in direction of flow, and deviation from the desired geometry. Thus this diffuser works, and apparently quite well for the problem of diffusing swirl; however, no conclusion can yet be drawn that this is the best geometry.

VI. RECOMMENDATIONS

I strongly recommend continuation of the test program. Perhaps with more information on the internal flow, the predictions of Jansen will be able to be used in the radial section of the diffuser (1).

First more study is needed on the present apparatus. Installation of a traversing mechanism across the inlet and solid support of the flat plate are of primary importance. Then the internal flow would have to be more carefully mapped. Hot-wire measurements should be taken to determine if axi-symmetry really exists.

Several modifications to the apparatus could be done next within one year. The radius could be reduced in at least two successive steps. New fan blades in the induced draft fan would give a greater axial flow rate if the pitch could be decreased. At least one centerbody could be tried.

Future experiments could try changed wall geometry. It appears from the first tests that an interior streamline of the free jet (Figure I) would be an improvement.

VII. APPENDIX

APPENDIX A

Description of Apparatus and Methods of Construction

The apparatus consisted of a model diffuser based upon a hypothetical reversing gas turbine. The hypothetical turbine had a four-inch-diameter exhaust. The model was constructed three times actual size to reduce the velocities involved. It thus had a one-foot-diameter inlet. The flat plate was made of acrylic-plastic sheet one-half-inch thick. The curved wall shape was to be screeded from wet plaster. A plenum was constructed around the diffuser to allow suction from an induced-draft fan. The swirl-inducing mechanism was placed outside and below the plenum upstream of the inlet section.

Materials chosen to do the construction were three-quarter-inch plywood for the plenum and support, slotted angle for frames and braces, plaster for the stream shape and acrylic plastic for the plate. Note the plans in Figure VI.-.

First, the supporting frame was constructed of slotted angle and the base of the plenum bolted to it. Then the support for the plaster cast was secured to the top of this table-like structure. Expanded metal lath was used on top of the plywood support to reinforce the plaster. There should be no trouble cutting the plaster, lath, and plywood at one time with a sabre saw when it is desired to reduce the radius. The plaster screed was mounted first with two bearings to a pipe held perpendicular to the table. The inlet hole in the table was left closed until plaster work was finished.

Using information obtained from U. S. Gypsum, Ultracal-60 high-strength plaster was selected for its long setting time and low expansion (8) (10). This plaster was found to have insufficient "period of plasticity" to work properly. One hundred pounds of this was used to form a base layer. Upon further consultation with U. S. Gypsum, it was decided that for this application Hydrocal-B-11 high-strength plaster would be more suitable. Some sodate retarder was also obtained

to attempt to extend the working time. The B-11 plaster was supposed to have a longer period of plasticity, although having also a faster setting time, less strength, and more expansion. Use of the retarder was found to produce cracking in amounts greater than one part liquid mix with five parts water. One part liquid retarder in twenty parts of water produced a period of plasticity of about half an hour ending about one hour after the plaster and water were mixed. The use of any retarder at all, however, caused a marked weakening of the plaster with attendant crumbling. Dehydration of the finish layer by the previous layers caused the finish layer to tear and set quickly. Wetting the surface or using an above-normal amount of water in the mix failed to correct this deficiency. A great part of this problem can be attributed to the mounting of the screed. The pipe support proved to be insufficiently rigid, and also prevented easy lifting of the screed from the surface of wet plaster. The screed should be firmly but adjustably mounted, the best method being with a point support at the center and a skid at the rim (9). It should be adjustable such that succeeding layers will cover the entire surface. This will allow the screed to be forced down on the plaster by hand (with adjustments fixed). An alternative method would be to lay the plaster in small strips, starting at the inlet and outlet, each strip being circular. Using no retarder and mixing plaster in small amounts, it might be possible to get a satisfactory surface. Due to the large size of the model and close tolerance desired of plus or minus five thousandths of an inch, plaster was abandoned in favor of paraffin. The smoothest plaster surface that could be obtained had low spots up to one-fourth inch. I feel that items of smaller diameter would be considerably easier to screed accurately. If the job could be done in two layers or even just three, the accuracy would be greatly enhanced in plaster. With wax, the working time was infinite, although the surface built up rather slowly. Carbon black was added to the paraffin to give a good photographic background. The melted wax was applied to the plaster with a paint brush, and the screed, now mounted on a skid, used to level the surface. Vertical surfaces were the hardest to cover completely, however, a satisfactory surface was at last achieved.

Rotating screens were selected to induce the swirl. These have

a quickly dissipating wake. A converging section downstream of the screens was meant to reduce the boundary layer and make the flow more uniform. The inlet section was constructed of plaster and expanded metal lath, coated with paraffin. The support for the screens was salvaged from the apparatus of Willem Jansen. Screen area was kept large for lower pressure drop. The screen used was stainless steel, 40 x 40 mesh, 43.6% open, with 0.0085"wire diameter. The outer screen was wired in place. The inner screen was connected by a "B" size V-belt to an one-half-horse-power variable-speed motor. The speed control on the motor allowed the inner-screen speed to be controlled from 110 to 1100 rpm. Upon operation it was found that the screen needed further support, and so an one-eigth-inch steel hoop was soldered around the inside of the rim at the top of the screen.

The acrylic plate was cut using a rotating table and band saw. It was supported from above by eighteen cap screws tapped to within one-sixteenth-inch of the lower surface. Pressure taps were made by drilling a 0.0465 inches hole within one-thrity-second of the lower surface, then drilling through with a 0.025 inches drill 0.050 inches. Brass tubing was forced into the hole in a tight fit. Traversing holes of three-eighths inch diameter were made, then plugged and the plug surface lapped smooth.

The first pressure taps in the plaster surface were made in an unusual manner. Frist two strips of ten tubes each were buried just below the surface of the plaster. It was expected that the tubing would show through the translucent plaster, but this was not the case. With the addition of wax there was no possibility of locating the tubes visually. Thus test holes were drilled until one of the tubes was hit. Using the direction of the tubing and the relative location of other adjacent tubes, the remaining taps were relatively easy to drill into. Soap and water verified that each tube connected to only one pressure tap. The first data obtained showed strange oscillations in the static pressure. When the lower taps were tested for leaks, it was found that there was considerable communication between tubes and to the atmosphere, apparently due to the porosity and cracking of the plaster. A second complete

set of taps was made using brass plugs, driven into oversize holes, through the entire wax, plaster, and plywood support. These had 0.025-inch holes drilled in them and tubing attached to the other side. The plugs were sealed and a new surface over them formed with wax. Testing this time showed no leaks.

The induced-draft fans available in the laboratory were rated at a pressure of three inches of water. When one fan was connected to the apparatus, it stalled and was unable to pull air through the apparatus. The solution was to put two fans in series, thus obtaining approximately a six-inch rating, which was sufficient for the job. Plywood doors were installed at the inlet to the induced-draft fans to control the flow rate. These could be held in any position using a bolt and slot, and could be adjusted from outside the plenum chamber. These doors formed a throttle valve, allowing no leakage to atmosphere.

It was found that the plywood was too flexible to hold an accurate position of the acrylic plate relative to the bottom of the diffuser. Thus four three-quarters inch spacers were added at the rim to ensure the correct gap was obtained.

Tufts of thread were placed on several radius lines on both the flat and curved surfaces. The tufts were placed on the acrylic plastic surface using small pieces of vinyl tape. On the wax surface the tufts were knotted to threads every two inches, and the threads attached to plywood with tape at their ends. These tufts gave an immediate overall picture of the surface flow, and could be photographed from above the apparatus with a four-by-five-inch plate-film camera.

The apparatus was now ready to take data at its largest radius.

APPENDIX B

SAMPLE DATA

The following is a set of static tap readings with an inclined Merriam oil manometer board, s.g. = 0.827, at 25°.

Screen RPM	C	T2	T4	T6	T8	T10	T12	T14	T16
2000	- 3.0	- 2.9	- 2.7	- 1.9	- 0.5	0.2	0.7	0.8	0.8
2500	- 1.5	- 1.5	- 1.3	- 0.5	- 0.5	0.6	1.0	0.9	0.9
3000	- 0.6	- 0.6	- 0.2	- 0.1	- 0.6	1.0	1.3	1.1	1.1
3500	2.4	2.5	2.9	0.3	- 0.3	1.6	1.7	1.4	1.3
4000	3.3	3.6	3.4	0.3	- 0.1	1.8	1.8	1.6	1.4
4500	4.3	4.6	3.9	0.3	- 0.1	1.9	1.9	1.7	1.5
5000	4.3	4.7	4.0	0.4	0.0	2.0	2.0	1.7	1.6

T18	T20	T22	T24	E0	E2	E4	E6	E8	B8
0.6	0.3	0.0	0.0	- 1.0	- 1.8	- 1.4	- 0.6	1.1	2.1
0.7	0.4	0.2	0.0	- 1.0	- 1.8	- 1.1	- 0.1	1.9	3.0
0.8	0.5	0.2	0.0	- 1.1	- 1.9	- 1.0	0.4	2.9	3.4
1.0	0.6	0.3	0.0	- 1.0	- 1.5	- 0.1	2.1	5.2	3.8
1.0	0.6	0.3	0.0	- 0.9	- 1.4	0.2	2.8	5.7	4.0
1.1	0.6	0.3	0.0	- 0.8	- 1.3	0.6	3.4	6.1	4.2
1.1	0.7	0.3	0.0	- 0.8	- 1.3	0.6	3.5	6.2	4.3

B10	B12	B14	B16	B18	B20	B22	B24
1.2	1.1	1.1	1.2	1.0	0.7	0.1	0.0
1.6	1.3	1.3	1.3	1.1	0.8	0.2	0.0
1.9	1.5	1.5	1.5	1.2	0.8	0.2	0.0
2.5	1.9	1.7	1.7	1.3	0.9	0.2	0.0
2.7	2.0	1.9	1.8	1.4	1.0	0.3	0.0
2.8	2.2	2.0	1.9	1.5	1.0	0.2	0.0
2.9	2.2	2.1	2.0	1.5	1.1	0.3	0.0

p_a	corr.	T	W.B.	D.B.	hum.	p_{cone}
29.946	- 0.139	80.0°	57.5	80	22%	1.35

Below is a sample traverse.

Screen RPM	p_{cone}	p_a	corr.	T	W.B.	D.B.	hum.	r	
5000	1.4	30.186	-0.125	75.0	56	73.5	30%	10^{11}	
bottom	0.05	0.10	0.15	0.20	0.25	0.30	0.35	0.40	0.45
				1.1	1.6	1.8	2.1	2.4	2.8
0.50	0.55	0.60	0.65	0.70	0.75	0.80	0.85	0.90	0.95
3.0	3.3	3.6	3.8	4.0	4.3	4.6	4.8	5.0	5.5
1.0	1.05	1.10	1.15	1.20	1.25	1.30	1.35	1.40	1.45
5.7	5.8	6.0	6.1	6.4	6.8	7.0	7.0	7.1	7.2
1.50	1.55	1.60	1.65	1.70	1.75	top			
7.2	6.8	6.4							

APPENDIX C

Sample Calculations

CALIBRATION OF FLOW-METER CONE

Bernoulli Equation of a Streamline for Incompressible Flow:

$$\frac{1}{2}(C_2^2 - C_1^2) + \frac{p_2 - p_1}{\rho} + g(h_2 - h_1) = 0$$

Becomes for a Pitot Tube:

$$C_1^2 + \frac{2}{\rho}(p_2 - p_1)$$

$$\rho = \frac{w}{g}$$

From Mark's Handbook, pg. 14 - 67

$$w = 1.325 \quad \frac{p_a}{T}$$

p_a = barometric pressure in inches of Hg.
T = atmospheric temperature in °R.

$$p_2 - p_1 = \frac{(h_2 - h_1)_{oil}}{12} \times \text{sp.gr.oil} \times \sin(\text{manometer slope}) \times w_{H_2O}$$

$$= (h_2 - h_1)_{oil} \quad \frac{.827 \times \sin 5° \times 62.4}{12}$$

$$c = \sqrt{\frac{2g}{w} \frac{.827 \times \sin 5° \times 62.4}{12}} \quad \sqrt{\Delta h}$$

Velocity was measured at the mean of five equal areas, then averaged.

For a nozzle:

$$c = \frac{C_D}{\sqrt{1 - (\frac{A_2}{A_1})^2}} \quad \sqrt{\frac{2g \ \Delta p}{w}}$$

The average velocity indicated by the pitot traverse should be the same as that indicated by the cone when the proper value of C_D is used. Mach effects are not present over 1% at these velocities. Using two different flow rates, the discharge coefficient was determined.

$$C_D = \bar{c} \sqrt{\frac{1 - (\frac{A_2}{A_1})^2}{\frac{2g \ \Delta p}{w}}} = 0.788$$

This value was used with the cone pressure to determine the bulk flow rate of the diffuser.

REYNOLDS SIMILARITY

$$Re = \frac{\rho c D}{\mu}$$

$$Re = 3.41 \times 10^5$$

	PROTOTYPE		MODEL
T	1200°F./1660°R.		70°F./530°R.
μg	2.7×10^{-5}	lbm/ft.sec.	1.23×10^{-5}
ρg	0.0239	$lbm/ft.^3$	0.0750
D	1/3	ft.	1 ft.
c_x	578	ft./sec/.	84.0 ft./sec.
C_θ	1000	ft./sec.	145.7 ft./sec.
c	1156	ft./sec.	168 ft./sec.

These velocities are not rigid but show the approximate center of the range of interest.

NON-DIMENSIONALIZING PRESSURE READINGS

Measured velocity 155 ft./sec. at R = 0.5

Screen speed = rpm.motor x pulley ratio x π x dia. of screen

$$= 4000 \times \frac{2.2}{10.0} \times \pi \times \frac{24.375}{12}$$

$$= 5600 \text{ ft./min.}$$

$$= 93.3 \text{ ft./sec.}$$

Measured bulk velocity 42.7 ft./sec.

$$C_\theta = \frac{155}{93.3} \cos 15.9° \times \text{screen speed}$$

$$= 0.0373 \text{ rpm. screen}$$

For test series, bulk velocity = 76.6 ft./sec.

$$c_{in} = c_x^2 + C_\theta^2$$

$$C_D = \bar{c}\sqrt{\frac{1-(\frac{A_2}{A_1})^2}{\frac{2g\ \Delta p}{w}}} = 0.788$$

This value was used with the cone pressure to determine the bulk flow rate of the diffuser.

REYNOLDS SIMILARITY

$$Re = \frac{\rho cD}{\mu}$$

$$Re = 3.41 \times 10^5$$

	PROTOTYPE		MODEL
T	1200°F./1660°R.		70°F./530°R.
μg	2.7×10^{-5}	lbm/ft.sec.	1.23×10^{-5}
ρg	0.0239	$lbm/ft.^3$	0.0750
D	1/3	ft.	1 ft.
c_x	578	ft./sec/.	84.0 ft./sec.
C_θ	1000	ft./sec.	145.7 ft./sec.
c	1156	ft./sec.	168 ft./sec.

These velocities are not rigid but show the approximate center of the range of interest.

NON-DIMENSIONALIZING PRESSURE READINGS

Measured velocity 155 ft./sec. at R = 0.5

Screen speed = rpm.motor x pulley ratio x π x dia. of screen

$$= 4000 \times \frac{2.2}{10.0} \times \pi \times \frac{24.375}{12}$$

= 5600 ft./min.

= 93.3 ft./sec.

Measured bulk velocity 42.7 ft./sec.

$$C_\theta = \frac{155}{93.3} \cos 15.9° \times \text{screen speed}$$

= 0.0373 rpm. screen

For test series, bulk velocity = 76.6 ft./sec.

$$c_{in} = c_x^2 + C_\theta^2$$

= 90°	c_{in} = 76.6	$\frac{1}{2} c^2$ = 6.7	$\frac{1}{2} (c_{in}^2 - c_{out}^2)$ = 0
45.8°	106.9	13.04	7.34
39.4	120.7	16.62	9.92
34.4	135.7	21.0	14.3
30.4	151.4	26.1	19.4
27.1	167.8	32.1	25.4
24.5	184.3	38.7	32.0
22.3	201.8	46.4	39.7

$\frac{p_{out} - p}{\frac{1}{2} \rho c_{in}^2}$ used for plotted points.

EFFICIENCY

The efficiency is a measure of the approach of the diffuser to frictionless flow. The possible pressure to be recovered should be the difference between the inlet and outlet dynamic pressures, i.e.

$$\frac{1}{2} \rho (c_{in}^2 - c_{out}^2)$$

The outlet static is easy to measure, as this is the pressure at which the diffuser exhausts. The inlet static pressure presents more of a problem. The inlet is theoretically a potential vortex. We know that there must be a core in a real fluid however, since the singularity at the center of a potential vortex cannot exist in a real fluid. Thus the pressure distribution across the inlet will decrease from a high value at the wall to a low value at the core.

I first noted bulk velocity is about five times wall velocity. To get a meaningful static inlet pressure, I subtracted the dynamic pressure difference between the wall velocity and the swirl velocity. This involves two assumptions. The first is that the total head is constant across the inlet. The second is that the axial component of inlet velocity has a negligible effect on inlet static pressure compared to the angular, or swirl, component. The inlet pressure is then defined as

inlet wall pressure minus this dynamic pressure difference.

$$p_{in} = p_{wall} - \frac{\rho}{2}\left(\overline{C_\theta}^2 - C_{\theta wall}^2\right)$$

$$= p_{wall} - \frac{\rho}{2}\left[\overline{C_\theta}^2 - \left(\frac{\overline{C_\theta}}{5}\right)^2\right]$$

$$= 0.9 \cdot 1.819 - \frac{0.00228}{2}\left[34{,}700 - 1{,}387\right]$$

$$= -36.4 \text{ lbs./ft.}^2$$

The outlet pressure was used as reference and is thus 0.

A measure of efficiency is thus the percentage of dynamic-pressure difference between inlet and outlet recovered.

$$\eta = \frac{p_{out} - p_{in}}{\frac{\rho}{2}\left(c_{in}^2 - c_{out}^2\right)}$$

$$= \frac{-(-36.4)}{\frac{0.00228}{2}\left(201.8^2 - 76.6^2\right)}$$

$$= \frac{36.4}{39.7}$$

$$= 91.7\%$$

BIBLIOGRAPHY

1. W. Byron Brown and Guy R. Bradshaw, "Method of Designing Vaneless Diffusers and Experimental Investigation of Certain Undetermined Parameters," N.A.C.A. Tech. Note 1426, 1947;

2. Willem Jansen, "Steady Fluid Flow in a Radial Vaneless Diffuser," A.S.M.E. Paper No. 63-WA-12;

3. Tatsuji Kawaguchi and Yoshimasa Turaya, "The Rotating Flows in a Vaneless Diffuser Having Two Parallel Discs," Bull. of J.S.M.E., Vol.9, No. 36, (1966) p. 711 - 718;

4. J.R. Kettler, "Final Summary Report, Reversible Turbine Nozzle Development Program," Airesearch Mfg. Co. of Arizona Report No. PT-755-R, 1958;

5. Ronald C. Pampreen, "The Laminar Incompressible Boundary Layer in a Constant-Area Vaneless Radial Diffuser," A.S.M.E. Paper No. 66-WA/FE-3;

6. O. Ruchti, "Versuche mit Radialdiffusoren," Technische Berichte, Bd. 11, (1944) p. 129-133;

7. A.N. Sherstyuk and A.C. Sokolov, "Meridonal Profiling of Vaneless Diffusers," Thermal Engineering, Vol. 13 No. 2, (1966) p.64-69;

8. U. S. Gypsum, "Industrial Tooling with Hydrocal Gypsum Cements, Basic Fundamentals," U.S.G. Pamphlet IGL-124;

9. U. S. Gypsum, "Industrial Tooling with Hydrocal Gypsum Cements, Circular Shapes (Turning)," U.S.G. Pamphlet IGL-111;

10. U. S. Gypsum, "Tooling and Pattern Making Materials Guide," U.S.G. Pamphlet IGL-420.

Figure I

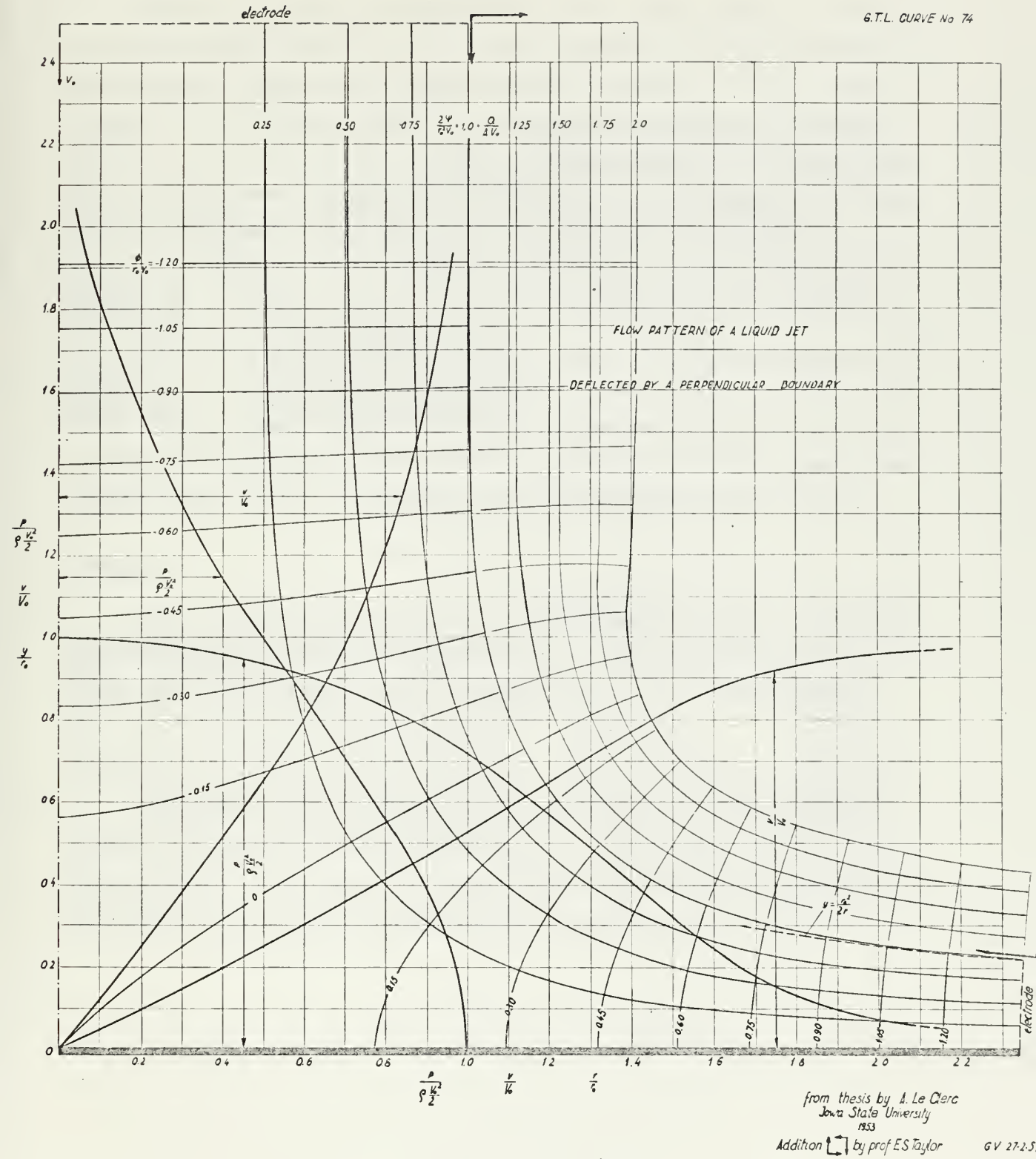
electrode
G.T.L. CURVE No 74
FLOW PATTERN OF A LIQUID JET
DEFLECTED BY A PERPENDICULAR BOUNDARY
from thesis by A. Le Clerc
Iowa State University
1953
Addition by prof E.S. Taylor
GV 27-2-5

FIGURE II

The picture gives an overall view of the test apparatus. Flow was radially inward through rotating screens, upward and outward through the test section to the square plenum chamber. Two axial flow fans were attached to the plenum chamber in series and can be seen in the background. Downstream of the fans were a settling chamber, honeycomb, and cone used for measuring mass flow. To the left of the apparatus is the inclined-oil-manometer board used for measurement of pressures.

FIGURE III

This picture shows the rotating screens and drive arrangement. The screens rotated in a groove on the plywood plate at the top. Only the inner of two screens was rotated in this experiment. The screens were clamped in supporting aluminum plates. Rotation at different speeds was accomplished using the variable-speed half-horse-power motor shown.

FIGURE IV

The top of the apparatus was acrylic plastic to allow viewing the flow. Access plugs were provided every two inches and can be seen at the lower left. The pressure taps and their tubing are at lower right.

FIGURE V

This shows the curved surface of the diffuser. The surface was formed by rotating the metal-edged plywood screed shown around a central support which is not shown. At upper right pressure taps can be seen. At lower left are the threads to which tufts were attached.

Figure II

Figure III

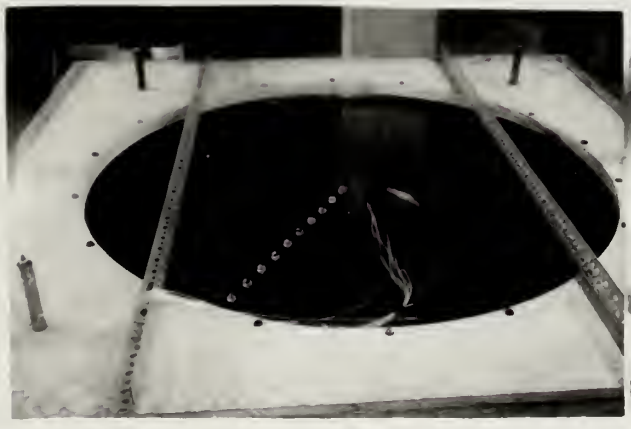

Figure IV

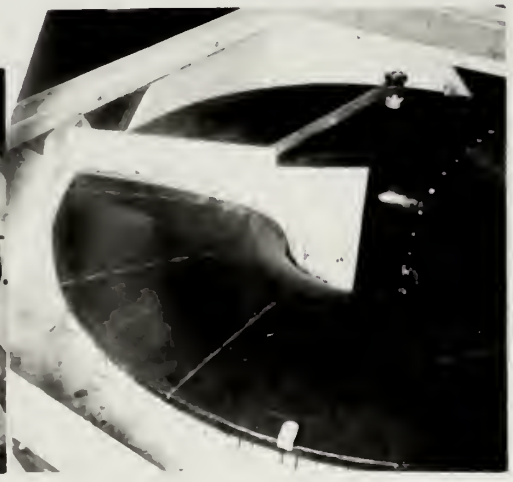

Figure V

Figure VI

Apparatus Plans

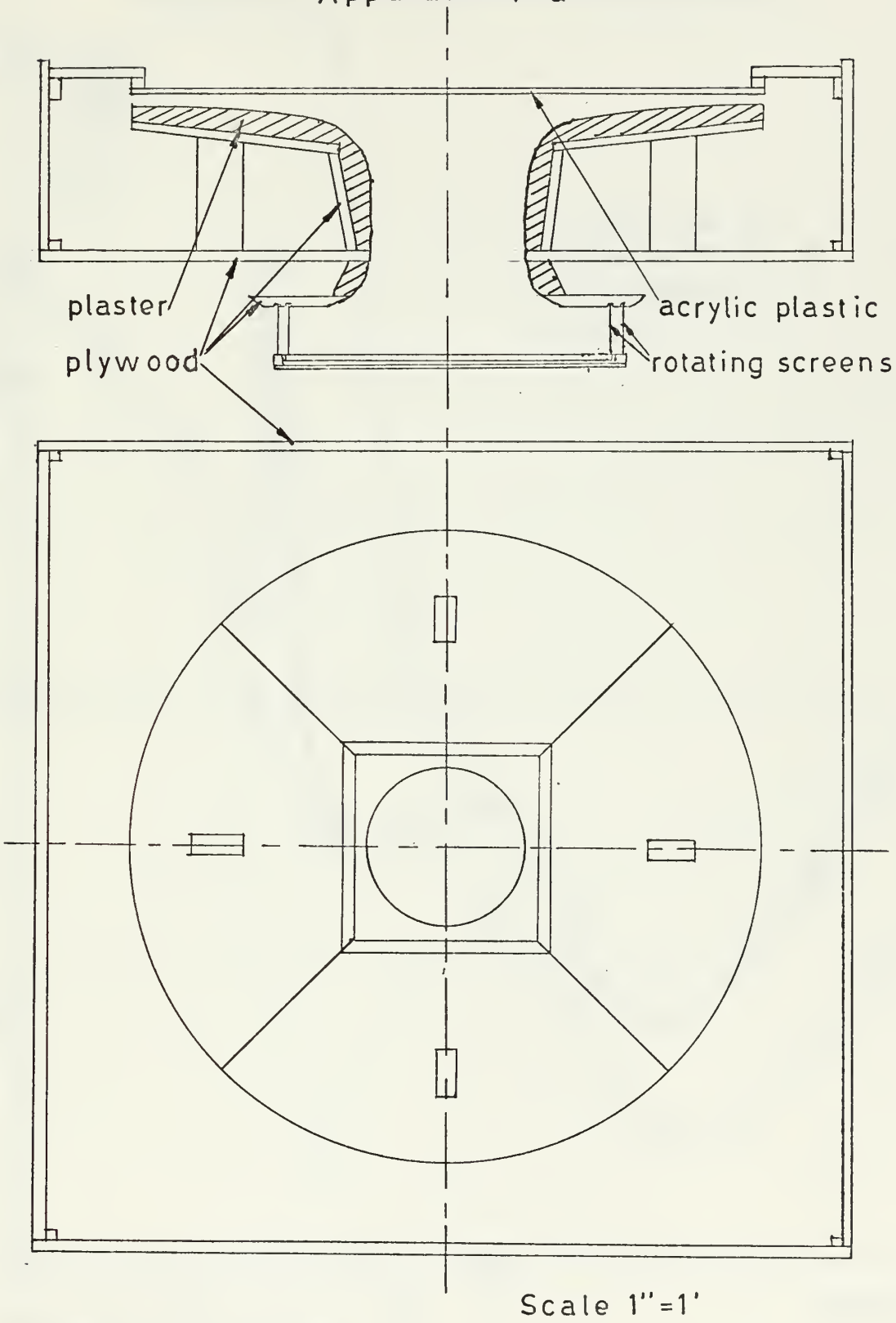

Scale 1"=1'

Figure VII

Wall Static Pressure vs. Radius, $\alpha = 90°$

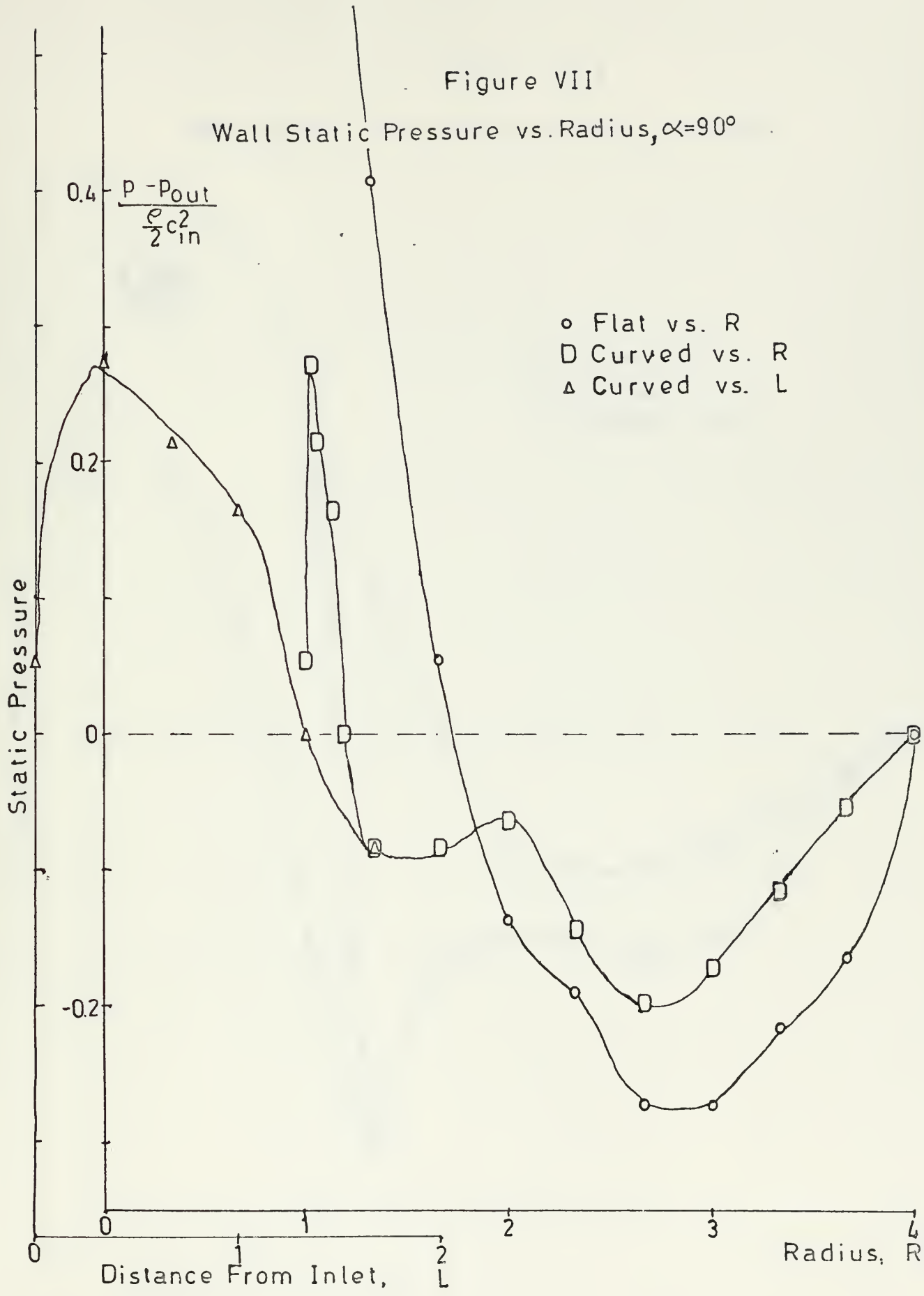

Figure VIII

Wall Static Pressure vs. Radius, α=45.8°

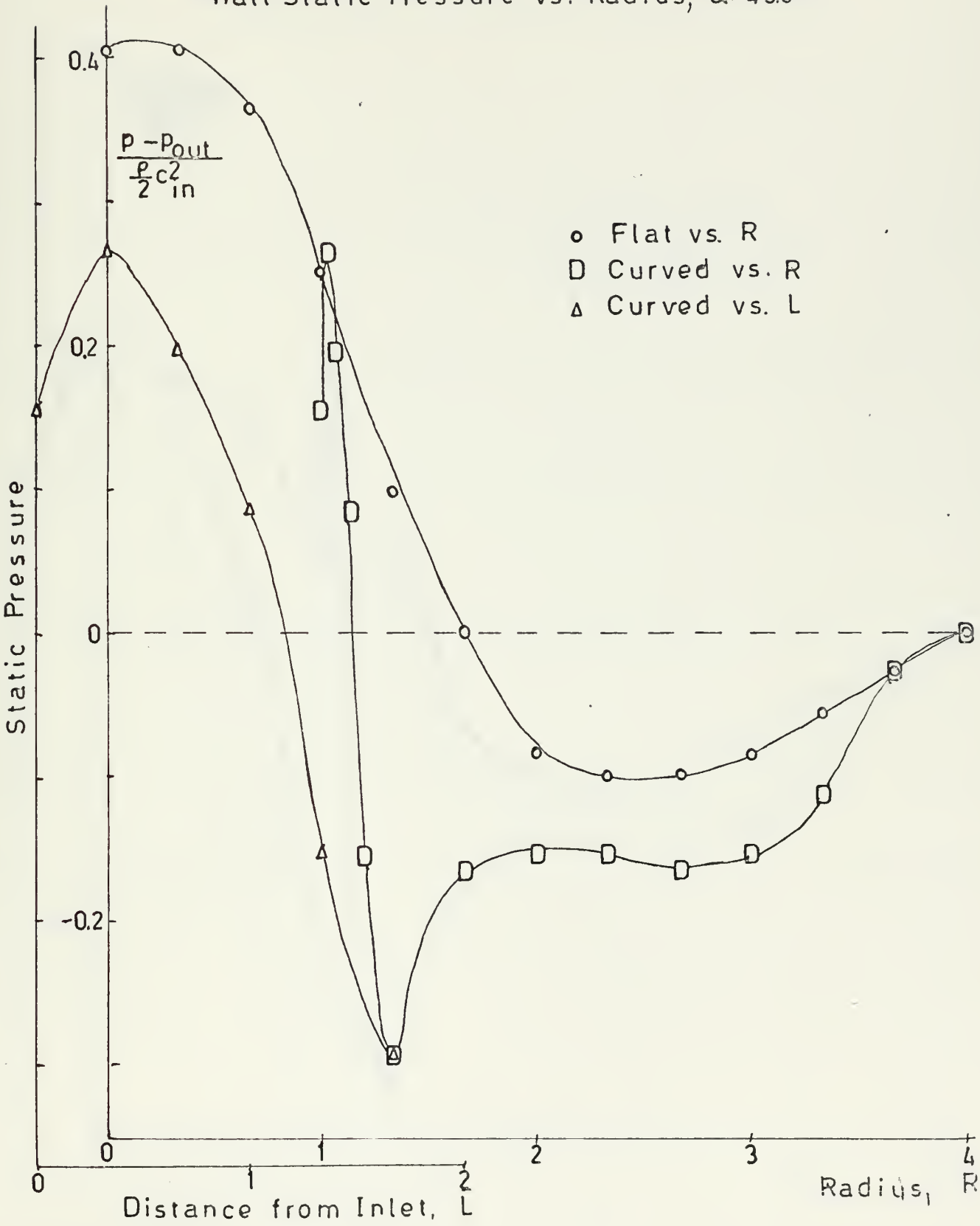

Figure IX

Wall Static Pressure vs. Radius, $\alpha = 39.4°$

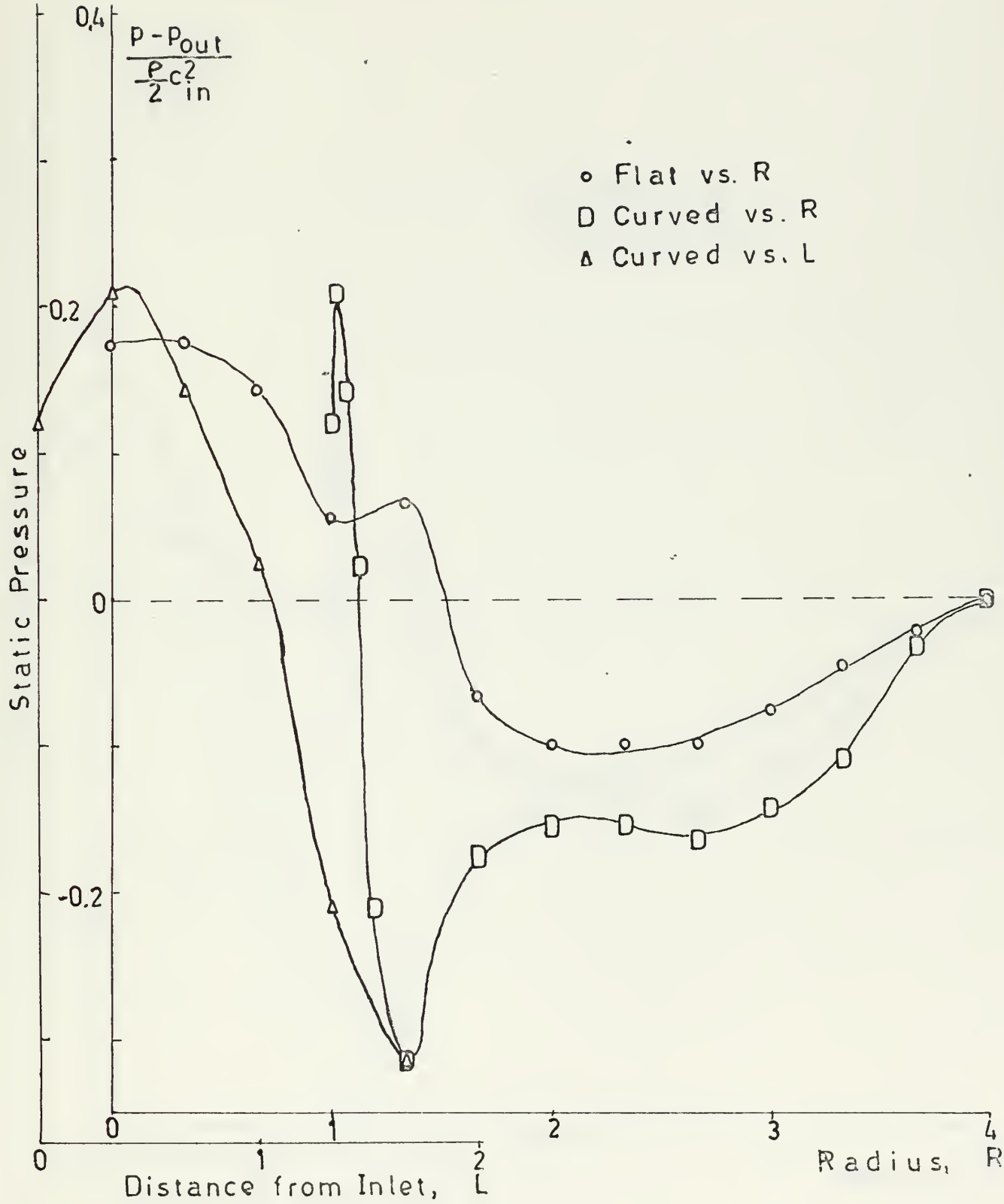

Figure X

Wall Static Pressure vs. Radius, $\alpha = 34.4°$

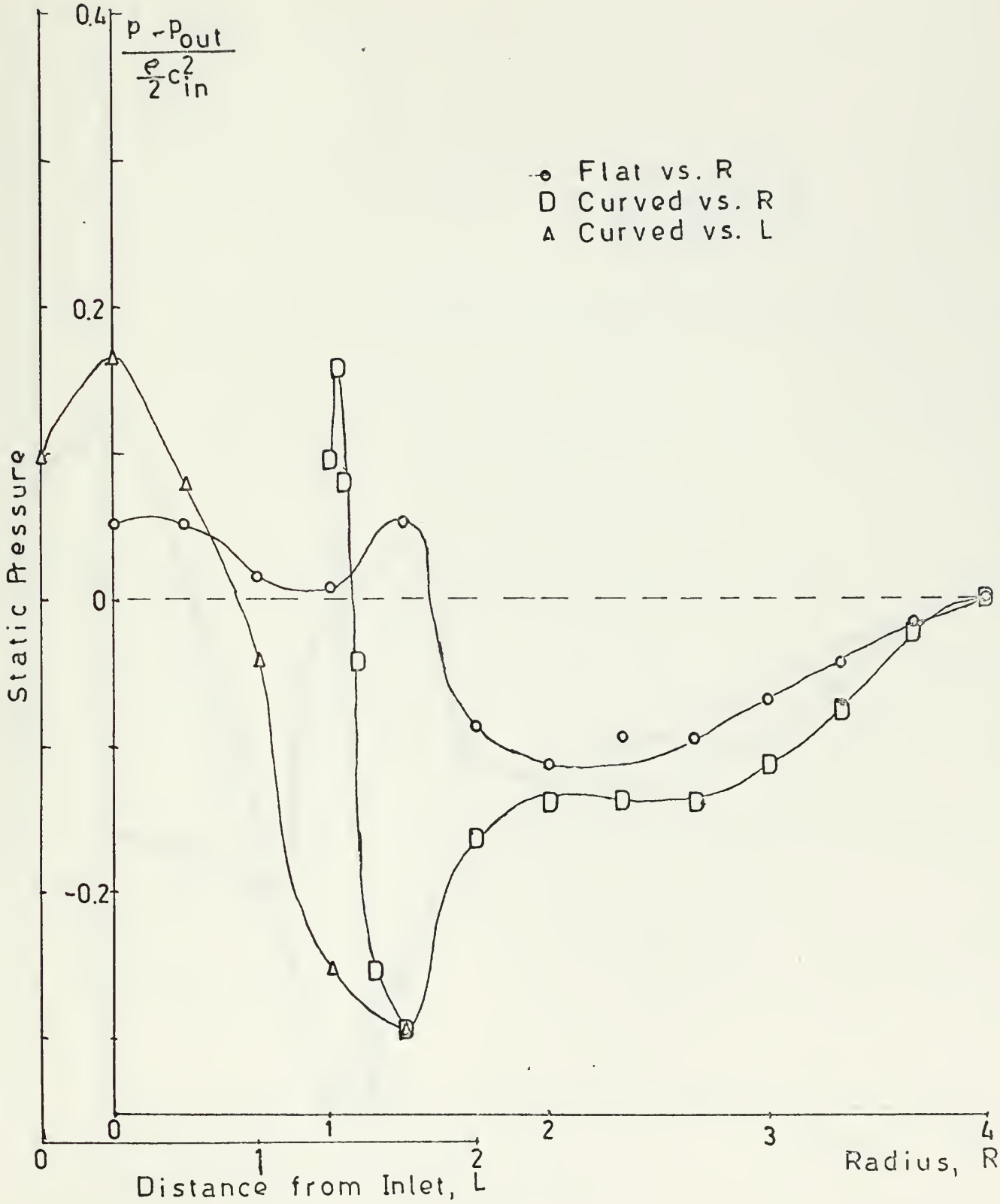

Figure XI

Wall Static Pressure vs. Radius, $\alpha = 30.4°$

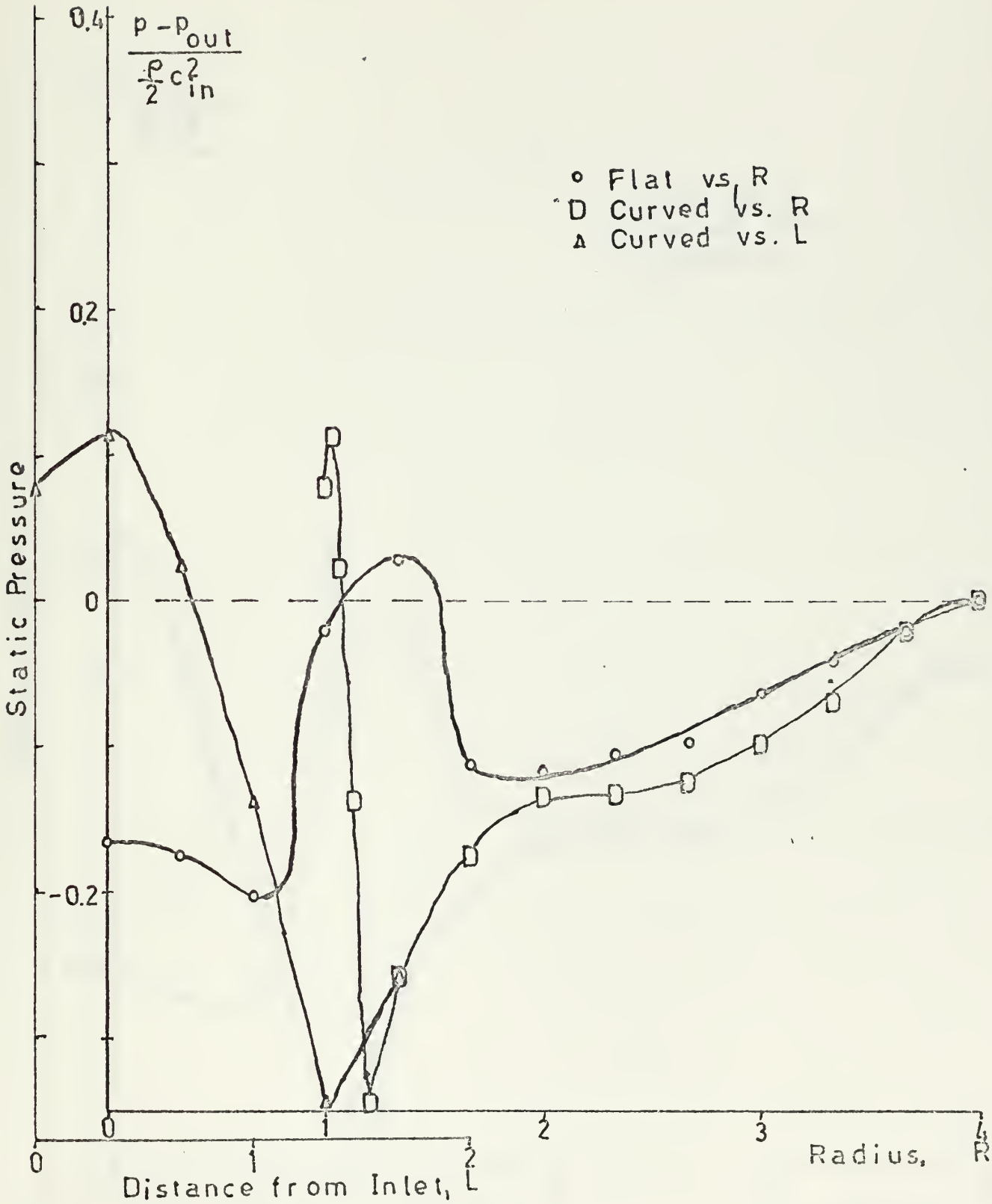

Figure XII

Wall Static Pressure vs. Radius, $\alpha = 27.1°$

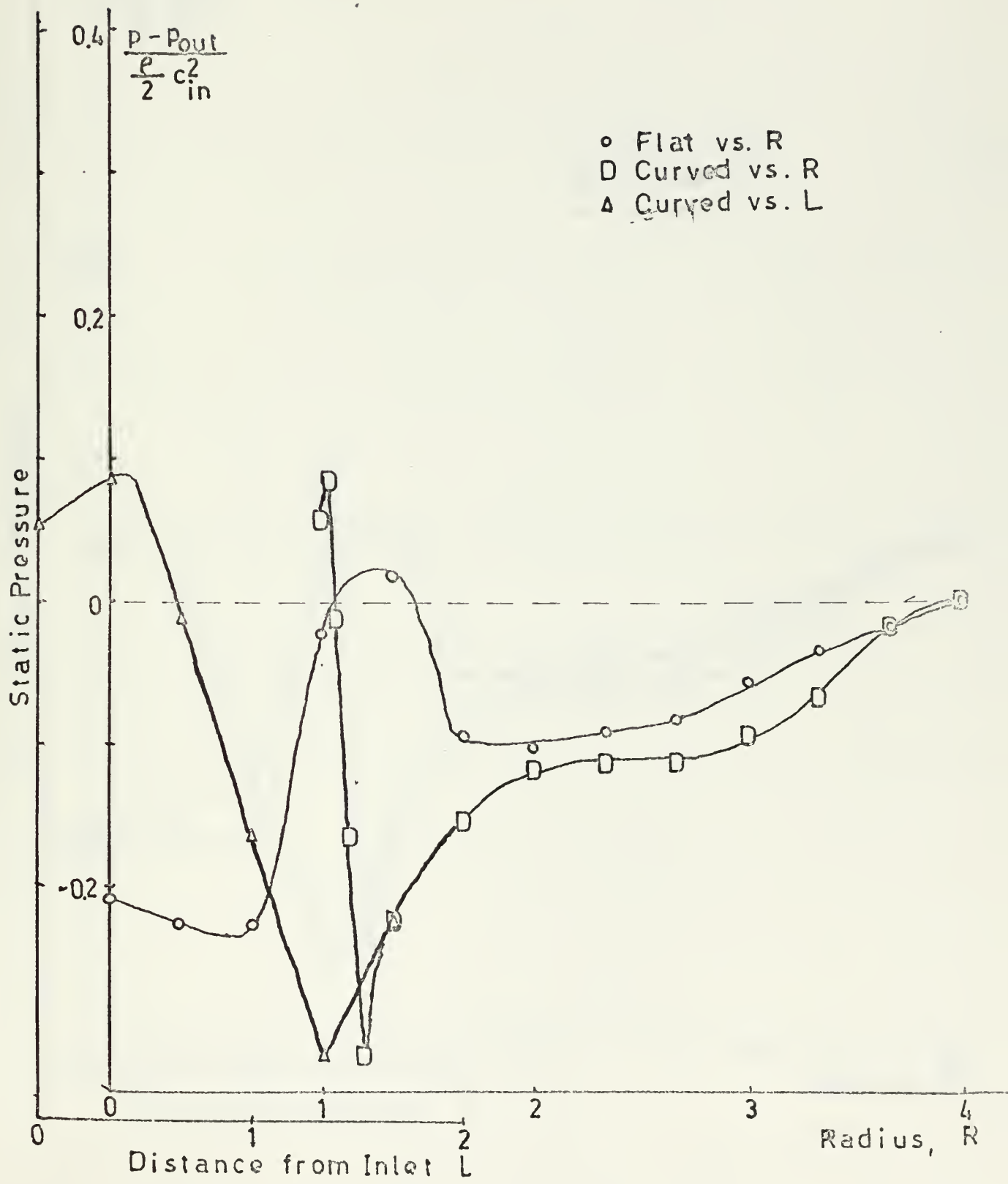

Figure XIII

Wall Static Pressure vs. Radius. $\alpha = 24.5°$

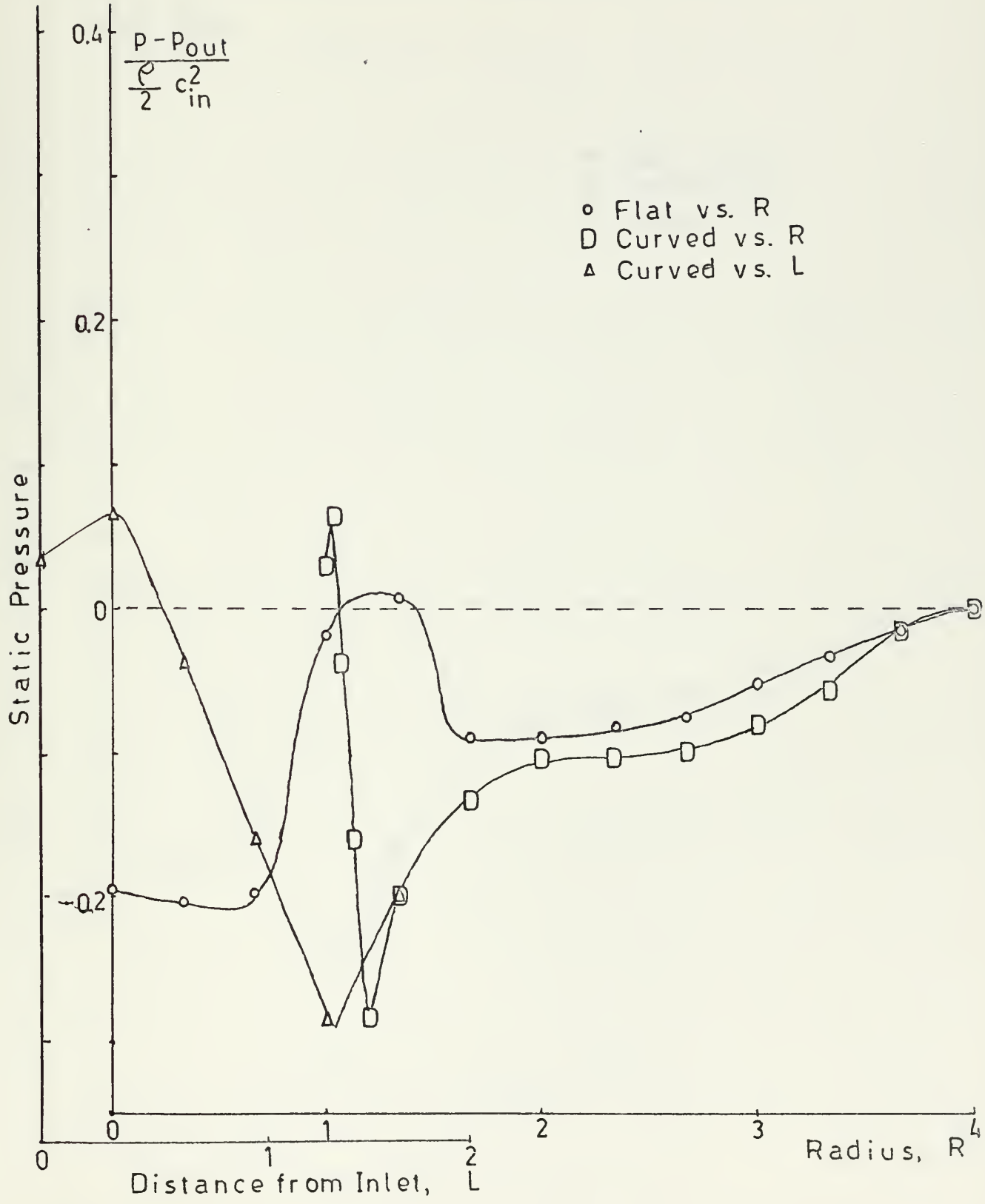

Figure XIV

Wall Static Pressure vs. Radius, $\alpha = 22.3°$

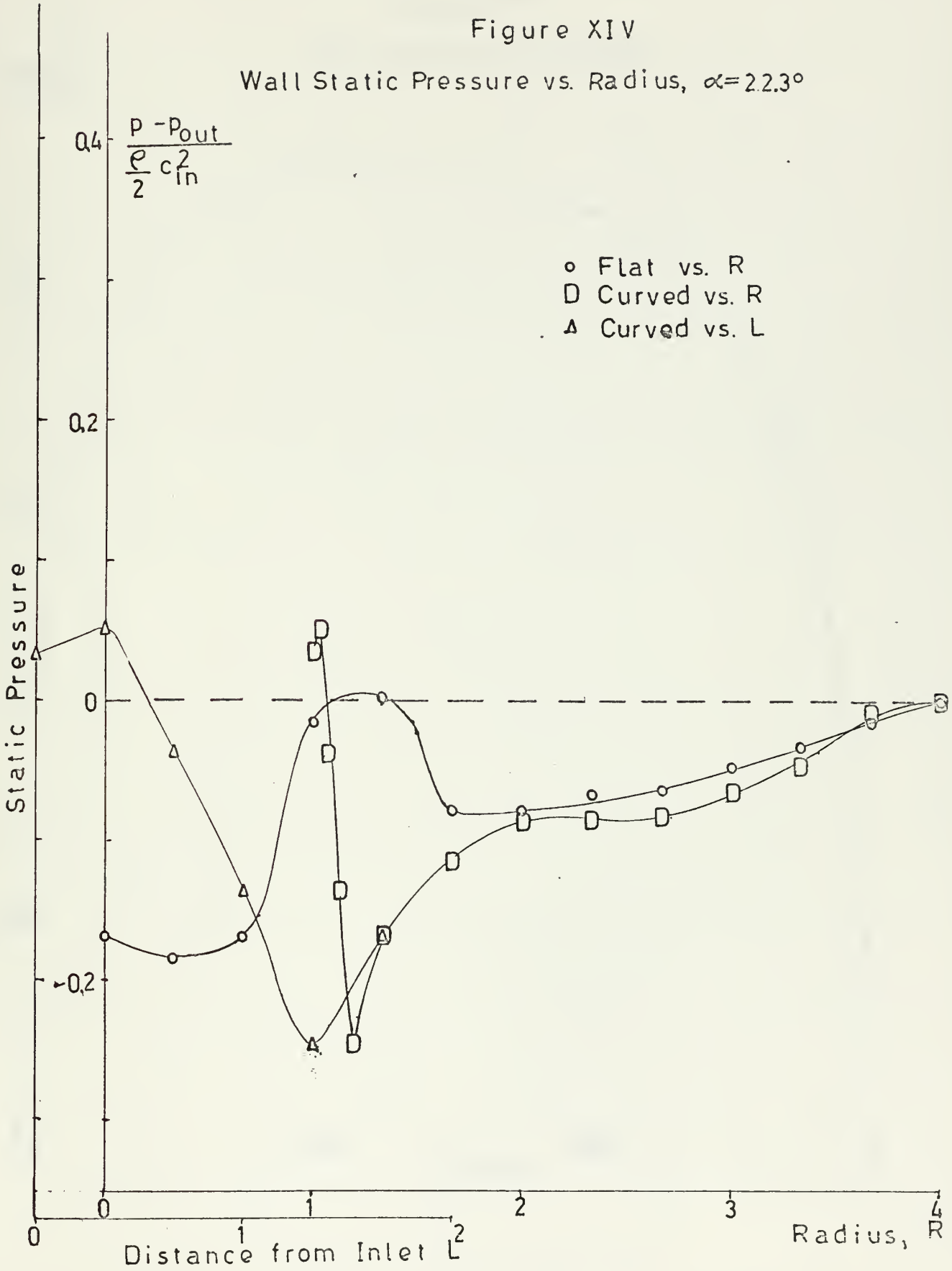

Figure XV

Inlet Velocity, $\alpha = 24.4°$

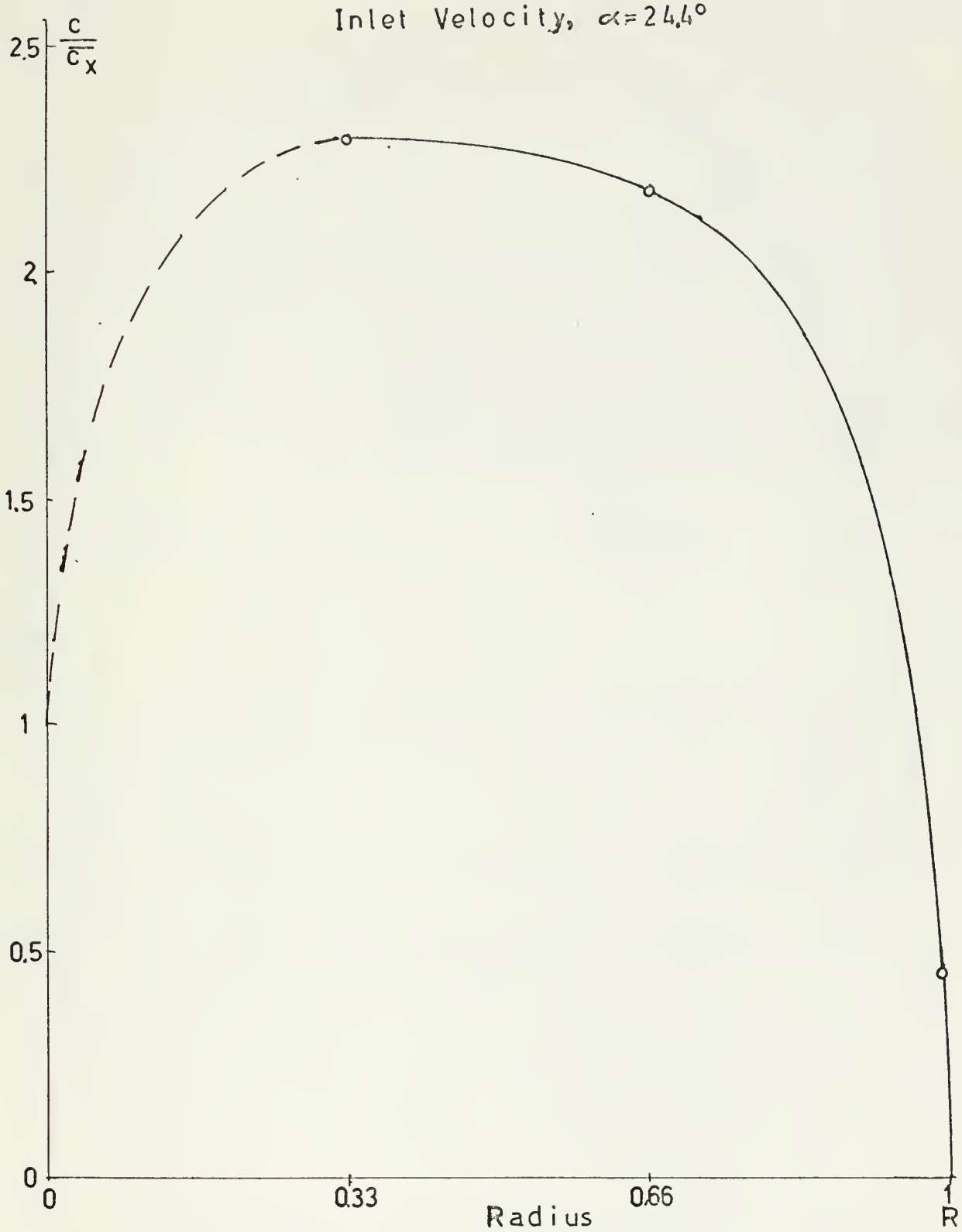

Figure XVI

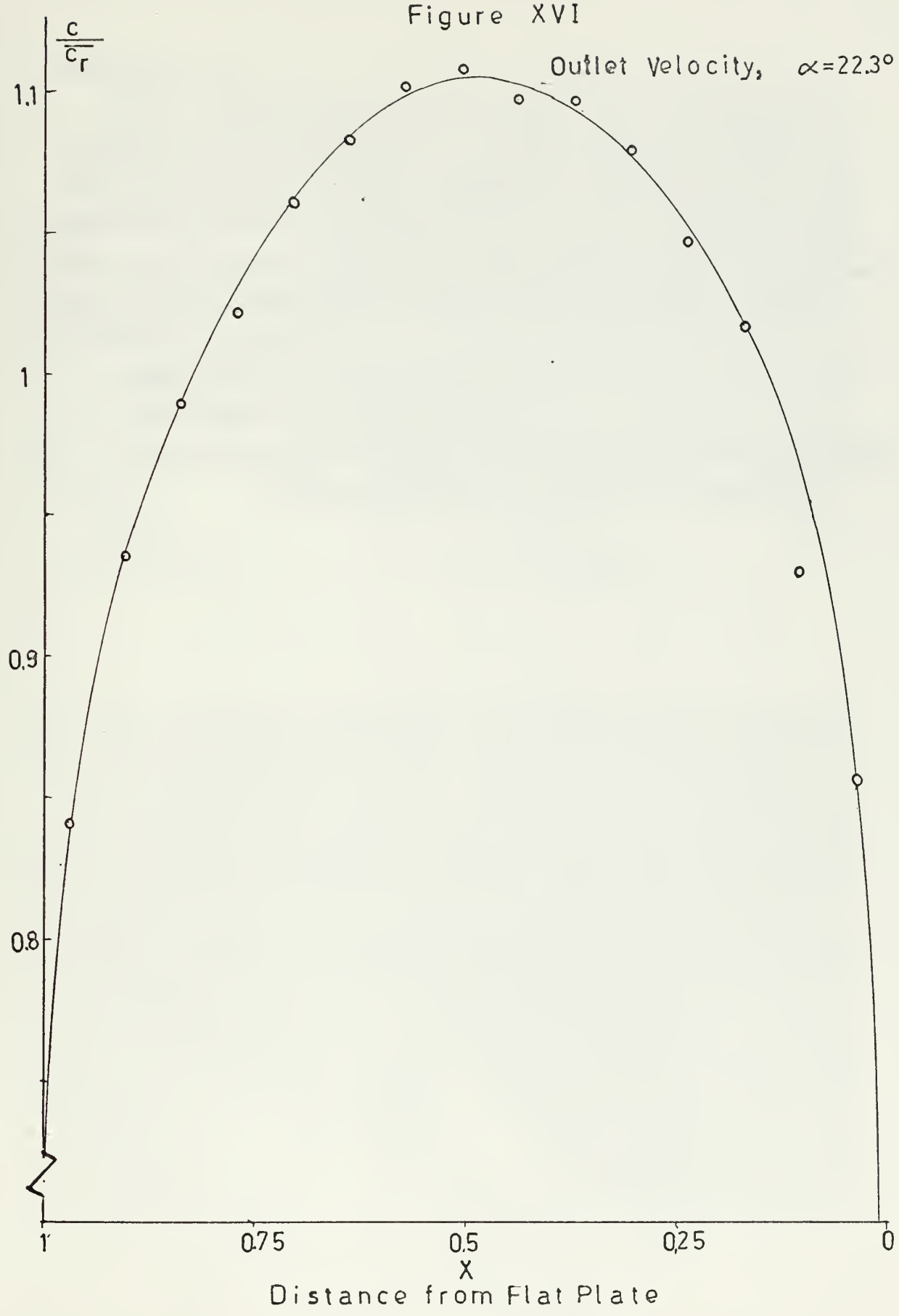
c/c_r
Outlet Velocity, α=22.3°
1.1
1
0.9
0.8
1
0.75
0.5
0.25
0
X
Distance from Flat Plate

FIGURES XVII - XX

These photographs show the tuft pattern while the diffuser is operating. The air enters at the upper-right corner and leaves at the left side and bottom. The tufts attached to strings are on the curved surface while those taped on are on the flat plate. Tufts on the flat plate near the upper-right corner of the photographs, which corresponds to the diffuser center-line, are hard to see because they oscillate through such a large arc.

FIGURE XVII is at alpha equals 32.2°.

FIGURE XVIII is at alpha equals 21.4°.

FIGURES XIX and XX are both at alpha equals 24.7°, Figure XX being a close up of the outer section of the diffuser.

Figure XVII

Figure XVIII

Figure XIX

Figure XX

Figure XXI

Efficiency vs. Inlet Swirl Angle

ACCOPRESS®